Transfer of Gases at Natural Air-Water Interfaces[1]

WAYNE J. BRTKO[2] AND ROBERT L. KABEL

Center for Air Environment Studies, The Pennsylvania State University, University Park 16802

(Manuscript received 14 June 1977, in final form 13 March 1978)

ABSTRACT

The natural exchange of gases across an air-water interface is an important mechanism that can be quantified. The mass-transfer coefficients characterizing the liquid phase can be predicted using certain models representing the liquid phase turbulence. Methods have been developed to approximate the necessary input parameters. Predictions of the models yielded liquid-phase mass-transfer coefficients well within an order of magnitude of experimental data at air-water interfaces.

1. Introduction

The exchange of gases between the atmosphere and underlying bodies of water is receiving increased attention in order to understand natural phenomena taking place within the environment. This is especially so in recent years due to growing concerns over environmental pollution and the subsequent movement of atmospheric pollutants. Many of these pollutants are ultimately transferred across the natural air-sea interface. One method of characterizing this process is to use a macroscopic approach, such as is described below.

The vertical flux F_g of a species in the atmosphere is given by

$$F_g = k_g(Z)[C_g(Z) - C_g(0)], \quad (1)$$

in which $k_g(Z)$ is the gas-phase mass-transfer coefficient and $C_g(0)$ and $C_g(Z)$ are the concentrations of the species in the atmosphere at the free liquid surface and at a height Z, respectively. If the gas phase concentration at a particular height is known by measurement or model prediction and the mass transfer coefficient can be obtained for the same height from a correlation, the vertical flux can be calculated as will be shown. A similar equation can be written relating the vertical flux F_l of the species in a water body to the vertical concentration driving force by

$$F_l = k_l(z)[C_l(0) - C_l(z)]. \quad (2)$$

In this equation, $k_l(z)$ is the liquid-phase mass-transfer coefficient and $C_l(0)$ and $C_l(z)$ are the concentrations of the species in the water body at the free liquid surface and at a depth z, respectively. Again, $C_l(z)$ is found by measurement or model prediction and $k_l(z)$ is obtained from a correlation. In this paper height increases positively upward and depth increases positively downward with $Z = z = 0$ at the air-water interface. Also capital letters are used for coordinate positions and velocities in the atmosphere and correspondingly lower case letters are used in the aqueous phase.

At steady state, the flux must be continuous across the air-sea interface, so that

$$F_g = F_l. \quad (3)$$

Equating (1) and (2) leaves two unknowns, the gas and liquid interfacial concentrations. A relationship between these variables is obtained by postulating equilibrium of phases at the interface. The validity of this postulate is well documented. The relation to describe this situation depends on the particular species of interest, but in many cases it would essentially be a solubility relation, such as

$$C_g(0) = HC_l(0), \quad (4)$$

where H is Henry's law constant. This constant has been experimentally determined for many chemical species at various temperatures and concentration levels.

Therefore, if $C_g(Z)$ and $C_l(z)$ are known or can be predicted and if $k_g(Z)$ and $k_l(z)$ can be determined by correlation, Eqs. (1)–(4) can be solved simultaneously for the interfacial concentrations and the desired vertical flux of the species of interest into or out of a body of water. Correlations for predicting values of $k_g(Z)$ are numerous in the field of meteorology. Kraft (1977) reviews many of them. In this paper, an attempt will be made to provide useful correlations for the liquid-phase mass-transfer coefficient $k_l(z)$. With the required input parameters, one can then quantify the natural process of mass

[1] CAES Publication No. 471-77.

[2] Present affiliation: E. I. duPont de Nemours and Co., Inc., Parkersburg, WV.

0022-3670/78/0543-0556$07.00

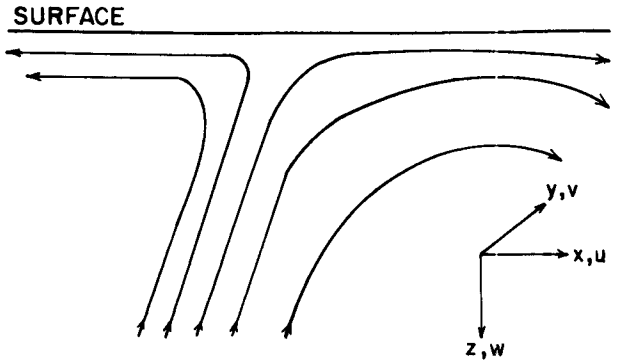

FIG. 1. Physical representation of a large eddy near a free liquid surface.

transfer between the atmosphere and underlying bodies of water. The ideas expressed here were developed by the authors and first put forth by Kabel (1975).

2. Liquid-phase mass-transfer-coefficient models

The earliest model useful for determining the liquid-phase mass-transfer coefficient for gas absorption by a turbulent liquid was presented by Whitman (1923). This was the film theory in which it is postulated that adjacent to the free liquid surface there exists a stagnant film below which the liquid is well mixed. It is assumed that mass is transferred through this film by molecular diffusion. The film then represents the major resistance to the transfer of mass into the liquid phase. The liquid phase mass transfer coefficient in this theory is given by

$$k_l = D/d_f, \tag{5}$$

where D is the molecular diffusivity of the species of interest in the liquid phase and d_f the thickness of the hypothetical stagnant film.

The next model proposed for the liquid-phase mass-transfer coefficient was the penetration theory (Higbie, 1935). In this model, the mass transfer process is characterized by molecular diffusion into fluid elements transported from the bulk liquid to near the free liquid surface by turbulent eddies. The diffusion of mass into the fluid elements occurs for a prescribed time θ_c which is assumed to be uniform for all turbulent eddies. The mass transfer coefficient is then given by

$$k_l = 2(D/\pi\theta_c)^{1/2}. \tag{6}$$

Danckwerts (1951) proposed the surface renewal theory by considering that there should be a random age distribution of fluid elements rather than a uniform contact time. The fractional rate of replacement of the fluid elements belonging to any age group is assumed to be equal to the surface renewal rate. Molecular diffusion into the fluid elements at the surface is again described by Higbie's penetration mechanism to yield the mass transfer coefficient

$$k_l = (Ds)^{1/2}, \tag{7}$$

where s is the surface renewal rate.

Hanratty (1956) and Perlmutter (1961) have developed modified penetration-surface renewal theories and Dobbins (1956), Toor and Marchello (1958), Harriot (1962) and Marchello and Toor (1963) have presented combinations of the film and penetration theories. Kishinevsky (1955) and King (1966) have proposed an alternative approach to the development of liquid-phase mass-transfer-coefficient models. In this approach, the concept of an eddy diffusivity, which parallels the molecular diffusivity, is employed in the liquid-phase mass-transfer-coefficient expression.

All of the models discussed so far retain one basic limitation in their present forms. While they can be used to interpret important experimental observations, great difficulties remain in applying them to predict liquid-phase mass-transfer coefficients. This is due to the fact that all of them contain one or more arbitrary parameters (e.g., d_f, θ_c and s), which cannot be specified *a priori* from the experimental conditions of a situation of interest. Therefore, the models require the correlation of experimental data to obtain an empirical relation for the arbitrary parameter. More importantly, the empirical relation must be determined for every different situation due to inadequate correlations. To resolve these problems, Fortescue and Pearson (1967) and Lamont and Scott (1970) have developed liquid-phase mass-transfer-coefficient models which contain physical quantities characteristic of the liquid-phase turbulent-flow field. These are the large eddy model and the eddy cell model.

a. Large eddy model (Fortescue and Pearson, 1967)

In this model, it is postulated that large eddies in the liquid phase are most effective in the mass transfer process of gas absorption by a turbulent liquid. These large eddies transport fresh fluid from the bulk turbulent liquid to near the free liquid surface (Fig. 1). Mass is transferred to these fluid elements by molecular diffusion. Then the solute-enriched fluid elements plunge back into the bulk of the turbulent liquid. This eddy motion is modeled with a sequence of roll cells, which are taken to be distributed as shown in Fig. 2. The roll cells move as a whole with the local mean surface velocity and are taken to be square. The dimension of the roll cells, which represents the characteristic length of the turbulent eddies, is taken to be in the integral length scale of the turbulent flow field.

The following arbitrary turbulent fluctuating velocity pattern is imposed within the roll cell:

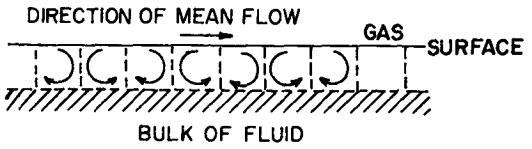

FIG. 2. Representation of roll cells near a free liquid surface.

$$\left.\begin{aligned} u &= A' \sin(\pi x/\Lambda) \cos(\pi z/\Lambda) \\ v &= 0 \\ w &= -A' \cos(\pi x/\Lambda) \sin(\pi z/\Lambda) \end{aligned}\right\}, \qquad (8)$$

where A' is a velocity scale and Λ the characteristic length of the eddies. The coordinate system is defined in Fig. 3. By definition, the mean mass-transfer coefficient of the roll cell is given as

$$\bar{k}_{rc} = \frac{-D}{(C_s - C_b)\Lambda} \int_0^{\Lambda} \left(\frac{\partial C}{\partial z}\right)_{z=0} dx. \qquad (9)$$

In this equation, C is the point solute concentration, C_s the solute concentration at the surface and C_b the bulk concentration of the solute. Taking the velocity scale A' equal to twice the root mean square of the turbulent fluctuating velocities, Fortescue and Pearson obtained an expression for C and subsequently $\bar{k}_{rc}$ by solving the steady-state, two-dimensional diffusion equation applicable within the roll cell. The resulting expression for the liquid-phase mass-transfer coefficient was

$$k_l = 1.46(Du'/\Lambda)^{1/2}, \qquad (10)$$

where u' is the root mean square of the turbulent fluctuating velocity u.

The quantities of u' and Λ in (10) are characteristic of the turbulent flow field and can be determined for a situation of interest. It should be noted that

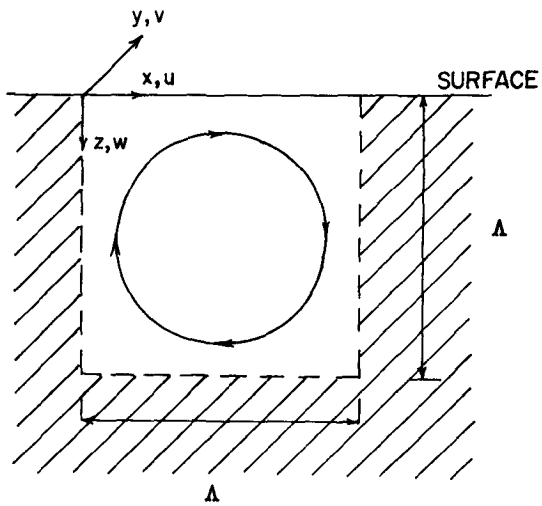

FIG. 3. A roll cell representation.

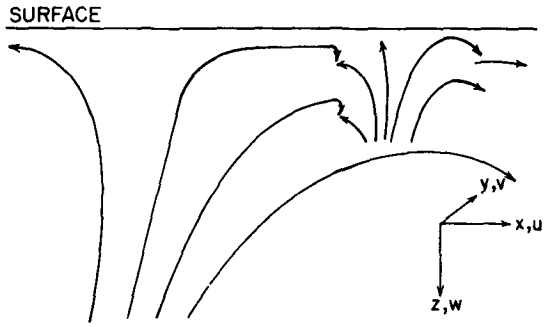

FIG. 4. A small eddy superimposed on a large eddy.

u' is a characteristic velocity and Λ a characteristic length, so that the ratio of these two parameters can be thought of as the surface renewal rate s. Therefore, (10) is really an extension of (7), in which the surface renewal rate has been specified in terms of physical quantities that can be measured.

b. Eddy cell model (Lamont and Scott, 1970)

As in the large eddy model, it is postulated that large eddies transport fresh fluid from the bulk of the turbulent fluid to near the free liquid surface. However, these eddies are assumed to have superimposed on them a similar motion on a much smaller scale (Fig. 4). Mass is transferred by molecular diffusion to the smaller eddies, which are considered to be most effective in the mass transfer process of gas absorption by a turbulent liquid.

The small-scale motions are characterized by idealized eddy cells as shown in Fig. 5. It is postulated that within the eddy cell exists a one-dimensional sinusoidal shearing motion of amplitude A at the mid plane of the entire cell. The dimension a of the eddy cell is taken to be the distance from the surface to the mid plane. Lamont and Scott's solution of the diffusion equation applicable in the eddy cell yielded

$$k_l' = 0.445(DA/a)^{1/2}, \qquad (11)$$

where k_l' is the mass-transfer coefficient for an idealized eddy cell.

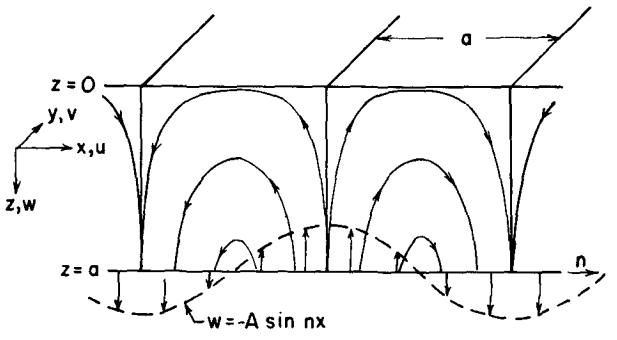

FIG. 5. Representation of viscous eddy cells near the liquid surface.

The dimension of the eddy cell and the amplitude of the shearing motion must be determined in order to apply (11). To accomplish this, the relative energies of the different scales of turbulent motion were examined using the turbulent energy spectrum. We first consider the turbulent fluctuating velocity w. This velocity can be decomposed into sinusoidal shearing motions of different amplitudes and different wavenumbers by performing a Fourier analysis on the turbulent velocity field. The turbulent energy spectrum function is based on this model of turbulence. Therefore, the energy spectrum, which indicates how the turbulent energy is distributed to any distinct wavenumber, then represents the energy of the component of the turbulent fluctuating velocity w corresponding to that distinct wavenumber. Also, the energy spectrum is then applicable for estimating the amplitude of the sinusoidal shearing motion for any distinct wavenumber.

In the eddy cell model, we used the Kovasznay energy spectrum (Hinze, 1959)

$$E(n) = 0.45\epsilon^{2/3}n^{-5/3}[1 - 0.6\nu n^{4/3}\epsilon^{-1/3}]^2, \quad (12)$$

where $E(n)$ is the turbulent energy spectrum function, ϵ the rate of turbulent energy dissipation per unit mass, ν the kinematic viscosity of the fluid and n the wavenumber. The amplitude of the sinusoidal shearing motion for any distinct wavenumber is given by

$$A = [nE(n)]^{1/2}. \quad (13)$$

The size a of the eddy cell corresponds to the wavenumber $n = \pi/a$ from the specification of the shearing motion in the cell.

Using (11), (12) and (13) and the above relation for a, Lamont and Scott obtained

$$k_l'(n) = 0.445(.45)^{1/4}\pi^{-1/2}\epsilon^{1/6}D^{1/2}n^{-2/3} \times [1 - 0.6\nu n^{4/3}\epsilon^{-1/3}]^{1/2}, \quad (14)$$

where $k_l'(n)$ is the contribution to the overall mass-transfer coefficient on a unit wavenumber basis, so that $k_l'(n) = k_l'/n$. Eq. (14) was finally integrated over the wavenumbers in the dissipation range to yield

$$k_l = 0.4D^{1/2}(\epsilon/\nu)^{1/4}, \quad (15)$$

where k_l is the liquid-phase mass-transfer coefficient for the eddy cell model.

The parameter ϵ is a calculable characteristic of the turbulent flow field. Although it is not obvious in (15), a portion can be thought of as a function of the surface renewal rate s. Hinze (1959), following Kolmogorov, gives $(\epsilon\nu)^{1/4}$ as a characteristic velocity and $(\nu^3/\epsilon)^{1/4}$ as a characteristic length for isotropic turbulence in the dissipation range under consideration. The ratio of these two characteristic parameters can be taken to be the surface renewal rate, yielding $(\epsilon/\nu)^{1/2}$. Therefore, (15) is an extension of (7), in which the surface renewal rate has been specified in terms of physical quantities that can be determined.

3. Determination of the input parameters for the models

The input parameters necessary in the large eddy and eddy cell models are difficult to obtain, requiring many detailed measurements of the variables characterizing the turbulence in the liquid phase. Some of the existing methods will be briefly discussed. Then less rigorous methods of determining the input parameters will be presented. These approximate methods greatly simplify the application of the models.

a. More rigorous methods

Ideally, for the large eddy model, the length scale of the large eddies can be taken equal to the depth at which the concentration is that of the bulk liquid. Unfortunately, this depth is not generally known. In this case, Λ can be determined using the mixing length hypothesis postulated by Prandtl (1925). This requires careful measurements of the turbulent fluctuating velocities near the surface of the water body and of the vertical profile of the mean fluid velocity. With the measured values of the turbulent fluctuating velocities, u' can also be specified for input into the large eddy model.

For the eddy cell model, the rate of turbulent energy dissipation is required. Careful measurements of the profiles of the turbulent velocities near the surface of the water body can be used to determine ϵ according to the relation (see Hinze, 1959)

$$\epsilon = \nu\overline{\left(\frac{\partial u_i}{\partial x_j} + \frac{\partial u_j}{\partial x_i}\right)\frac{\partial u_j}{\partial x_i}}, \quad (16)$$

where u_i and u_j are the turbulent fluctuating velocities in the x_i and x_j directions, respectively.

In practice, the values of the liquid-phase mass-transfer coefficient are desired for a number of different situations and using the above methods would require many detailed measurements for each situation. If that is so, one might as well measure the liquid-phase mass-transfer coefficients directly using the definition given in (2).

b. Approximation of input parameters

Rather than measure the liquid-phase mass-transfer coefficient for every situation of interest, it would be beneficial to have models that would allow its *a priori* determination under varied conditions. This capability would also allow more effective generalization of empirical results. For the large eddy model, one can use the same criteria as

O'Connor and Dobbins (1958) to approximate the input parameters. The root mean square of the turbulent fluctuating velocity can be taken equal to 10% of the mean fluid velocity and the length scale of the eddies can be taken equal to 10% of the total liquid depth. Another approximation, which seems more reasonable over a large range of applications, is to take u' equal to the liquid phase friction velocity w_* at the free liquid surface as postulated by Phillips (1966) and Kitaigorodskii (1973). For large, deep water bodies, using the above criterion for the length scale of the large eddies is unrealistic. In this case, this parameter can be taken equal to 10% of the depth of the wind mixed layer, which exists in many situations in large water bodies. This layer is considered to be a relatively turbulent region resulting from the transfer of momentum to the water body by the wind. The turbulence in this region should then promote mass transfer into the liquid. Kitaigorodskii (1973) gives the following empirical relation for the depth of the wind mixed layer:

$$d = C_E w_*/\Omega. \tag{17}$$

In this equation w_* is the liquid-phase friction velocity at the free liquid surface, Ω the Coriolis parameter is equal to $1.46 \times 10^{-4} \sin\lambda$, where λ is the latitude, and C_E is the dimensionless universal constant for the Ekman layer which was found equal to 10^{-1} by Charney (1969). Ths formulation presumes negligible thermally induced convection. Approximating u' by w_* is recommended in all cases. However, the approximation for Λ depends on the situation of interest. Therefore, the large eddy model expression for the liquid-phase mass-transfer coefficient becomes

$$k_l = 1.46(Dw_*/\Lambda)^{1/2}. \tag{18}$$

The rate of turbulent energy dissipation required in the eddy cell model can be approximated by performing a turbulent energy balance near the surface in the water body (see Kitaigorodskii, 1973). This balance is

$$\epsilon = -w_*^2 \frac{\partial u_w(z)}{\partial z} + \frac{g}{\rho_w}\overline{\rho' w'}, \tag{19}$$

in which w_* is the liquid phase friction velocity at the surface, $u_w(z)$ the mean fluid velocity at a depth z, g the gravitational acceleration, ρ_w the density of the liquid phase, and ρ' and w' the density and vertical velocity fluctuations. The term $-w_*^2[\partial u_w(z)/\partial z]$ is the rate at which turbulent energy is generated by the work of the Reynolds stress on the mean velocity gradient and is always positive. In (19), $g\overline{\rho' w'}/\rho_w$ is the rate of production of turbulent energy by the buoyant forces and is positive when there is a net buoyant flux upwards. Multiplication of (19) by $\kappa z/w_*^3$, where κ is the von Kármán constant usually taken equal to 0.4, yields

$$\frac{\kappa z\epsilon}{w_*^3} = -\frac{\kappa z}{w_*}\frac{\partial u_w(z)}{\partial z} + \frac{\kappa z g\overline{\rho' w'}}{w_*^3 \rho_w}. \tag{20}$$

In this equation, the last term is equal to the depth divided by a Monin-Obukhov length in the liquid phase, which is defined by

$$L_w = \frac{\rho_w w_*^3}{\kappa g \overline{\rho' w'}}. \tag{21}$$

The Monin-Obukhov length in the liquid phase represents the depth at which the magnitudes of the work done by the Reynolds stresses and by the buoyant forces are of the same order. Using the definition of L_w, Eq. (20) can be written as

$$\frac{\kappa z\epsilon}{w_*^3} = -\frac{\kappa z}{w_*}\frac{\partial u_w(z)}{\partial z} + \frac{z}{L_w}. \tag{22}$$

To permit the determination of ϵ from (22), an expression for the velocity profile, $u_w(z)$ in the body of water, is necessary. Phillips (1966) postulated the existence of a logarithmic velocity profile in water bodies under thermally neutral conditions. This has been supported experimentally by Shemdin (1972) in a wind tunnel and by Bye (1967) in observations of ocean drifts. The form of the velocity profile near the surface in the water body, modified to account for non-neutral conditions, is

$$u_w(0) - u_w(z) = \frac{w_*}{\kappa}\left[\ln\left(\frac{z}{z_{0w}}\right) + \frac{mz}{L_w}\right]. \tag{23}$$

In this equation, $u_w(0)$ is the surface drift velocity, z_{0w} a roughness depth and m a constant usually taken equal to 5. Differentiation of (23) with respect to the depth z in the liquid yields

$$\frac{\partial u_w(z)}{\partial z} = -\frac{w_*}{\kappa}\left(\frac{1}{z} + \frac{m}{L_w}\right). \tag{24}$$

This expression can then be substituted into (22) to obtain the relation

$$\epsilon = \frac{w_*^3}{\kappa}\left[\frac{1}{z} + \frac{(m+1)}{L_w}\right]. \tag{25}$$

One point should be made concerning the use of (25). Phillips (1966) has discussed limiting conditions on (23), which also apply to (25). These equations are adequate when $|z/L_w| < 0.1$ in stable conditions and $|z/L_w| < 0.03$ in the unstable case. At greater depths, the effects of buoyancy dominate over the Reynolds stress. By stable conditions, it is meant that there is a net buoyant flux downward which tends to dampen the turbulence in the liquid phase. The value of L_w as defined in (21) is then negative. When the liquid phase is unstable, there is a net

buoyant flux upward resulting in convective motions in the liquid and promotion of turbulence. The value of L_w is then positive. Between these two limits is the case of a thermally neutral liquid phase. In this case, the buoyant flux, which characterizes the flux of mass due to density differences, is zero. For neutral conditions, the parameter L_w then becomes infinite and the velocity profile is strictly logarithmic.

The rate of turbulent energy dissipation has been approximated and the resulting expression is given in (25). This relation can now be substituted into (15) to give the following eddy cell model expression for the liquid-phase mass-transfer coefficient:

$$k_l = 0.4D^{1/2}\left\{\frac{w_*^3}{\nu\kappa}\left[\frac{1}{z} + \frac{(m+1)}{L_w}\right]\right\}^{1/4}. \quad (26)$$

The liquid phase friction velocity w_* which appears in (18) for the large eddy model and in (26) for the eddy cell model, is not easily measured. However, it can be related to the gas phase friction velocity at the free liquid surface using the fact that the shear stress must be continuous there when there is no increase in wave motion. Brtko (1976) found conflicting evidence (both theoretical and experimental) in the literature on the importance of wave action to liquid-phase mass transfer. Thus in this work the free liquid surface was taken to be flat. Recent perspective on the matter is provided by Kondo (1976). Using the definitions of surface shear stress in both the atmosphere and a water body, then

$$\tau_a = \rho_a U_*^2 = \rho_w w_*^2 = \tau_w, \quad (27)$$

where τ_a and τ_w are the gas and liquid phase shear stresses, respectively, ρ_a and ρ_w are the gas and liquid phase densities, respectively, and U_* is the gas phase friction velocity at the surface. Rearrangement of (27) to solve for the liquid phase friction velocity yields

$$w_* = (\rho_a/\rho_w)^{1/2}U_*. \quad (28)$$

With this relation, (18) becomes

$$k_l = 1.46\left[\frac{DU_*}{\Lambda}\left(\frac{\rho_a}{\rho_w}\right)^{1/2}\right]^{1/2}, \quad (29)$$

and (26) becomes

$$k_l = 0.4D^{1/2}\left\{\frac{U_*^3}{\nu\kappa}\left(\frac{\rho_a}{\rho_w}\right)^{3/2}\left[\frac{1}{z} + \frac{(m+1)}{L_w}\right]\right\}^{1/4}. \quad (30)$$

Unlike the liquid phase friction velocity, the gas phase friction velocity can be determined due to advances in the field of meteorology. For thermally neutral flow over a rough surface, the well known logarithmic velocity profile exists in the atmosphere (Sutton, 1953; Munn, 1966). Panofsky (1963) has modified this profile to account for non-neutral conditions and has arrived at

$$U(Z) = (U_*/\kappa)[\ln(Z/Z_0) - \psi_m(Z/L)]. \quad (31)$$

In this equation, $U(Z)$ is the wind speed at a height Z, Z_0 is the roughness height of the underlying surface, $\psi_m(Z/L)$ is the departure from neutrality and L the Monin-Obukhov length in the gas phase. This length was defined by Monin and Obukhov (1954) as

$$L = -\frac{\rho_a c_p T_0 U_*^3}{\kappa g H_T}, \quad (32)$$

where c_p is the specific heat at constant pressure, T_0 the absolute atmospheric temperature and H_T the net upward heat flux. If the atmosphere is thermally neutral, this heat flux is zero and L, as defined in (32), is infinite. For stable conditions, the heat flux is negative indicating a net flux of heat downward in the atmosphere. This tends to dampen the turbulence in the atmosphere and L is positive. When the atmosphere is unstable, there is a net flux of heat upward, resulting in generation of turbulence. Then the heat flux is positive and L is negative.

Under stable conditions in the atmosphere, $\psi_m(Z/L)$ in (31) can be taken equal to $-\gamma_1 Z/L$, where Hicks (1973) suggests $\gamma_1 = 5.2$ and Businger *et al.* (1971) suggest $\gamma_1 = 4.7$. For unstable conditions, $\psi_m(Z/L)$ has been tabulated by Dyer and Hicks (1970) or can be approximated using the Hicks' (1973) relation

$$\psi_m(Z/L) = \exp\{0.032 + 0.448\ln(-Z/L) - 0.132[\ln(-Z/L)]^2\}. \quad (33)$$

Another parameter required for the application of (31) is the roughness height Z_0. Sutton (1953) has tabulated values of the roughness height, characteristic of various surfaces under neutral conditions in the atmosphere. Therefore, using these values in (31) and taking the Monin-Obukhov length equal to infinity, the gas phase friction velocity can be approximated for many situations as a function of the wind velocity at any reference height. An approach for determining Z_0 over water has been presented by Charnock (1955). In this case, Z_0 is taken to be a function of U_* such that

$$Z_0 = bU_*/g, \quad (34)$$

where g is the gravitational acceleration and b a constant equal to 0.016 (Wu, 1969). This empirical relation, which applies only under neutral conditions in the atmosphere, can be substituted into (31) with the Monin-Obukhov length taken equal to infinity. Then the resulting equation can be solved for U_* by trial and error.

When water is the underlying surface of concern, rather than specifying Z_0, correlations for the determination of the drag force on the surface are available. For example, Hicks (1973) gives the fol-

lowing expression for the drag coefficient under non-neutral conditions in the atmosphere:

$$C_D(Z) = [C_{D_N}(Z)^{-1/2} - \kappa^{-1}\psi_m(Z/L)]^{-2}, \quad (35)$$

in which $C_D(Z)$ and $C_{D_N}(Z)$ are the drag coefficients under non-neutral and neutral conditions, respectively. For $C_{D_N}(Z)$, Hicks (1973) has developed a correlation in terms of the wind speed at a reference height, i.e.,

$$C_{D_N} = [65 + 0.07U(Z)] \times 10^{-5}. \quad (36)$$

Finally, $C_D(Z)$ can be expressed in terms of the gas phase friction velocity such that

$$C_D(Z) = [U_*/U(Z)]^2. \quad (37)$$

Therefore, combining (35), (36) and (37) with the relations for $\psi_m(Z/L)$, the gas phase friction velocity can be obtained as a function of the wind velocity at any reference height.

There are other methods of determining U_* from the wind velocity. In order to be general and allow the possibility of choice, (29) and (30) will be left in terms of U_*, which can be obtained by the methods discussed or by other methods in the literature (Deacon and Webb, 1962; Sheppard, 1963). Then, U_* can be substituted as required in order to calculate the liquid-phase mass-transfer coefficient. One point should be made concerning (29) and (30). The gas-phase friction velocity and therefore the liquid-phase mass-transfer coefficient are both functions of the wind velocity. This is reasonable since the wind transfers momentum to the underlying water body thereby increasing the turbulence in the liquid phase. Since the rate of mass transfer across the free liquid surface is dependent on the turbulence in the liquid, the mass-transfer coefficient should be a function of the atmospheric wind speed. This has been verified experimentally in both the laboratory and the field, as will be shown.

4. Comparison of the predictions of the models with experimental evidence

a. Laboratory experiments

Fortescue and Pearson (1967) studied the absorption of carbon dioxide by water in turbulent channel flow. In their experiments, the turbulence was generated by a grid and was well represented by the correlations of Batchelor and Townsend (1948) developed from measurements on decaying turbulence downstream of a grid. Fortescue and Pearson (1967) and Lamont and Scott (1970) used (10) and (15), respectively, to predict liquid-phase mass-transfer coefficients representative of this experimental situation. The required input parameters for the large eddy and eddy cell models were

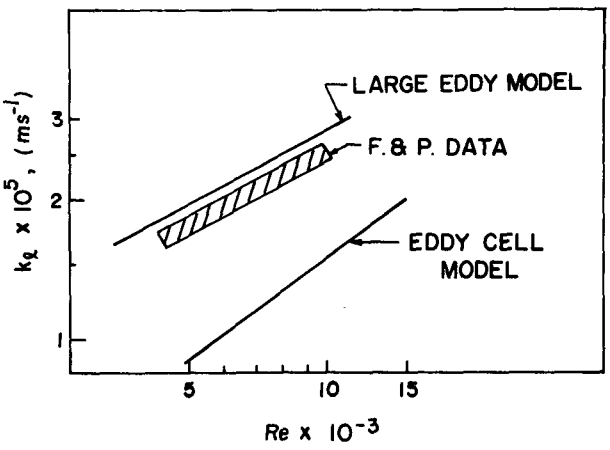

FIG. 6. Experimental and predicted liquid-phase mass-transfer coefficients in turbulent channel flow.

determined in each case. Comparison of the predictions of both models to the experimental values of the liquid-phase mass-transfer coefficient is shown in Fig. 6. The predictions of the eddy cell model are lower than the experimental results, while the predictions of the large eddy model are higher. Even though better agreement with the experimental data is observed for the large eddy model, the predictions of both models are within a factor of 2 of the measured values. Agreement of this quality is expected as well in other situations in which the input parameters can be obtained via a thorough characterization of the turbulence.

Liss (1973) obtained experimental values of the liquid-phase mass-transfer coefficient for absorption of oxygen into water in a wind tunnel. In these experiments, a rectangular tank was used to hold the water. The water was kept well mixed using a circulating pump and the depth of the water was maintained at 0.3 m. The wind velocity in the tunnel at a height of 0.1 m above the water surface was varied between 1.6 and 8.2 m s^{-1}. Liss determined the gas phase friction velocity U_* from measurements of the vertical logarithmic gas-phase velocity profile under thermally neutral conditions in the wind tunnel. He calculated the overall mass-transfer coefficient on a liquid phase basis with the definition

$$K_l = \bar{F}/[(C_g/H) - C_l]. \quad (38)$$

It appears that Liss used the oxygen concentration in the laboratory air for C_g and the initial undersaturated oxygen concentration in the water for C_l. His flux $\bar{F}$ appears to be calculated from the change in oxygen content in the recirculated water over the time period required for equilibration. This is tantamount to averaging the initial flux with zero, the flux at equilibration. Thus the experimental mass transfer coefficients may be a factor of 2 too low if the flux is linear with time. The factor can be even higher

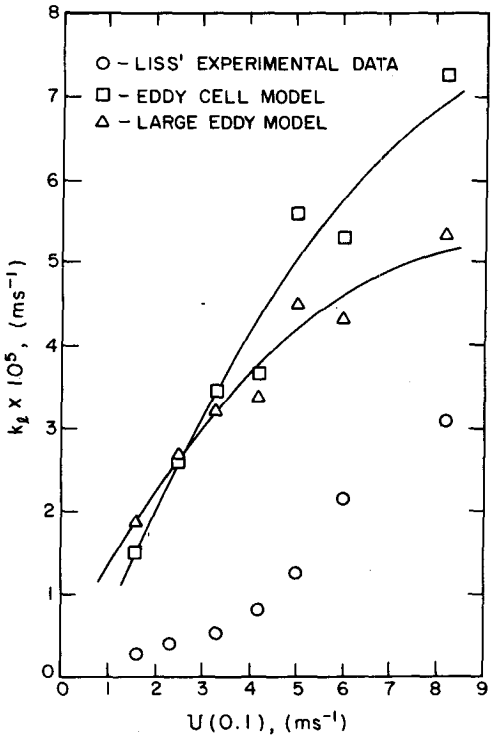

FIG. 7. Comparison of predicted liquid-phase mass-transfer coefficients to the experimental data of Liss (1973).

if the flux decays exponentially with time, which is more likely.

Liss' coefficient K_l is approximately equal to (or slightly less than) k_l in this case since the absorption of oxygen by water is a liquid phase controlled process due to the low solubility of oxygen. Model input parameters had to be approximated, so (29) and (30) were used to obtain the predictions. The experimentally determined values of U_* were substituted into the models and the necessary physical properties were taken at 298 K. In using the eddy cell model, the depth at which the liquid phase mass transfer coefficient was evaluated was taken to be 0.067 m. The problem involved in choosing this depth will be discussed later. For the large eddy model, the length of the eddies was taken to be 10% of the total depth of the water or 0.03 m. Neutral conditions ($L_w = \infty$) were assumed to exist in the liquid phase.

The experimental results and the predictions of the models are shown in Fig. 7. The predictions of both models are about three times higher than the experimental results and display an opposite curvature with wind speed. Both discrepancies may have resulted from the way the experimental fluxes were calculated. The predicted curvature is thought to be the more plausible and agrees with observations in the field. Liss (1975) and Kabel (1975) contemplate this matter further.

b. Field experiments

The next step is to compare the models to actual field data in which many other factors can affect the liquid-phase mass-transfer coefficient. Brtko (1976) has examined in detail many such experimental investigations. Most of them are unsuitable for evaluation of these models for reasons given in his thesis.

By far, the most appropriate experimental results for evaluation of the models are those obtained using the radon method (Broecker and Peng, 1971; Peng *et al.*, 1974). Due to the importance of this type of experiment in evaluating the models, the theory behind the radon method will be discussed.

Radon is generated within the sea by the decay of dissolved radium. As the partial pressure of radon produced in this manner greatly exceeds the partial pressure of radon in the sea which would be in equilibrium with the air above, escape of radon to the atmosphere takes place. The escape or flux F of radon into the atmosphere is described by

$$F = \frac{D}{d_f}\left(\frac{P_g}{H} - C_l\right), \tag{39}$$

in which P_g is the partial pressure of radon in the atmosphere, H Henry's law constant and C_l the radon concentration in the bulk liquid. A mass balance on a volume element at steady state yields

$$F_{\text{out}} - F_{\text{in}} = \int_0^\infty [\lambda_2 C^* - \lambda_1 C(z)]dz, \tag{40}$$

in which λ_1 and λ_2 are the radioactive decay constants for radon and radium, respectively. The term on the left-hand side is the difference between the flux of radon out of the volume element through a unit cross sectional area and the flux of radon into the volume element. Since the integration is over infinite depth, F_{in} may be taken to equal zero. Finally, $C(z)$ is the concentration of radon at any depth and C^* the concentration of radium, which is basically uniform with depth. Broecker *et al.* (1967) showed that well away from an air-sea interface, the rate of radioactive decay of radon is equal to that of its parent radium, so that $\lambda_2 C^* = \lambda_1 C(z)$ and the net flux equals zero in (40). This can be verified by substituting values of λ_2 (1.38×10^{-12} s^{-1}), λ_1 (2.08×10^{-7} s^{-1}) and C^* into (40). For C^*, the value of 1×10^{-13} g ℓ^{-1} reported by Riley (1971) for the mean concentration of radium in the oceans was used. This results in $C(z)$ being equal to 6.6×10^{-19} g ℓ^{-1}, which is essentially equal to the value of 6×10^{-19} g ℓ^{-1} reported by Riley (1971). If the no flux condition applied throughout the sea, Eq. (40) could be written

$$\lambda_2 C^* = \lambda_1 C_e, \tag{41}$$

in which C_e would be the radon concentration at any depth which would be in equilibrium with the existing radium. Eq. (41) can then be substituted into (40) to eliminate the radium concentration C^* and yield

$$F = \int_0^\infty \lambda_1[C_e - C(z)]dz. \qquad (42)$$

Intuitively, this says that the flux of radon is equal to the integrated deficiency of radon. By deficiency is meant the difference between the rate of decay of radon if there were no flux of radon and if there were a flux of radon.

The investigators obtained vertical concentration profiles for radon in the sea. The measured radon concentrations in standard units of disintegrations per minute per liter, are shown in Fig. 8. The solid lines represent the investigators' best curve fits to the data. The radon concentration in Fig. 8 increases with depth, as would be expected. In both of the investigations, the radium concentration in the liquid phase was also measured. This concentration was virtually constant with depth and was used to determine C_e in (42). Therefore, with the above information, (42) could then be solved for the flux of radon. The resulting values of the flux were then substituted into (39). In this equation, C_l is approximately 13 orders of magnitude greater than P_g/H for radon, so P_g/H was neglected. The value of C_l was obtained from the vertical radon concentration profiles in Fig. 8. Therefore, Eq. (39) could be solved for D/d_f or the overall mass transfer coefficient. The resulting values can be compared to the predictions from the eddy cell and large eddy models.

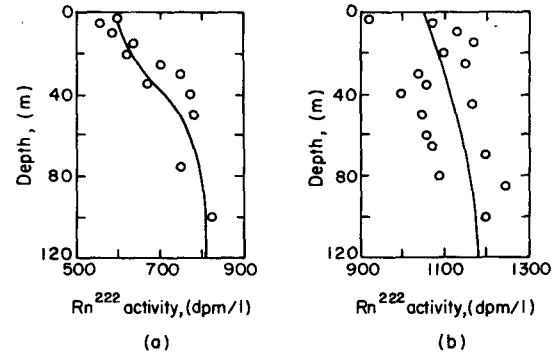

FIG. 8. Radon concentration profiles measured by (a) Broecker and Peng (1971) and (b) Peng *et al.* (1974).

Better than obtaining individual values of the overall mass transfer coefficient to compare to the predictions of the models, the data presented in Fig. 8 can be used to determine experimental values of k_l as a function of depth. First of all, the flux of radon at the surface determined by Broecker and Peng (1971) can be substituted into (39). Once again, P_g/H can be neglected. Then the radon concentrations from Fig. 8a can be substituted one at a time into (39). This procedure yields a vertical profile of the liquid-phase mass-transfer coefficient shown as data points in Fig. 9. The procedure can be repeated using the flux of radon determined by Peng *et al.* (1974) and the radon concentrations from Fig. 8b. The resulting vertical profile data of k_l are shown in Fig. 10.

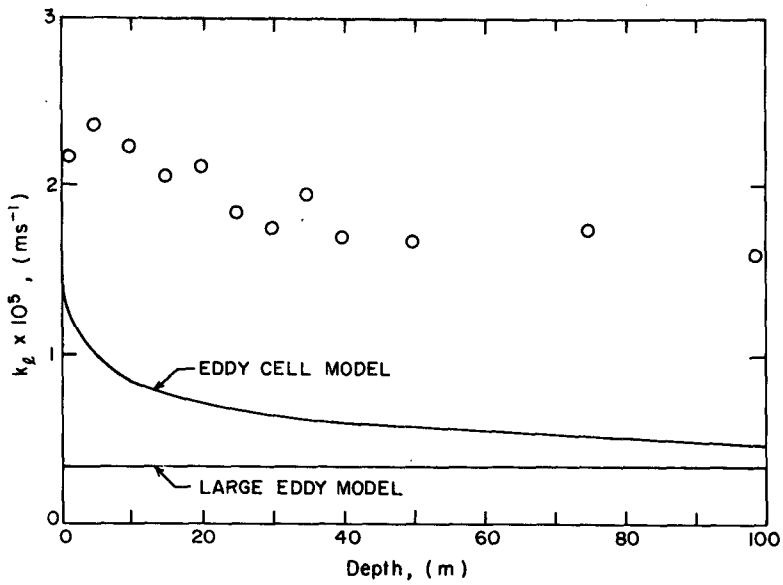

FIG. 9. Vertical liquid-phase mass-transfer-coefficient profiles from the work of Broecker and Peng (1971) and from the eddy cell and large eddy models.

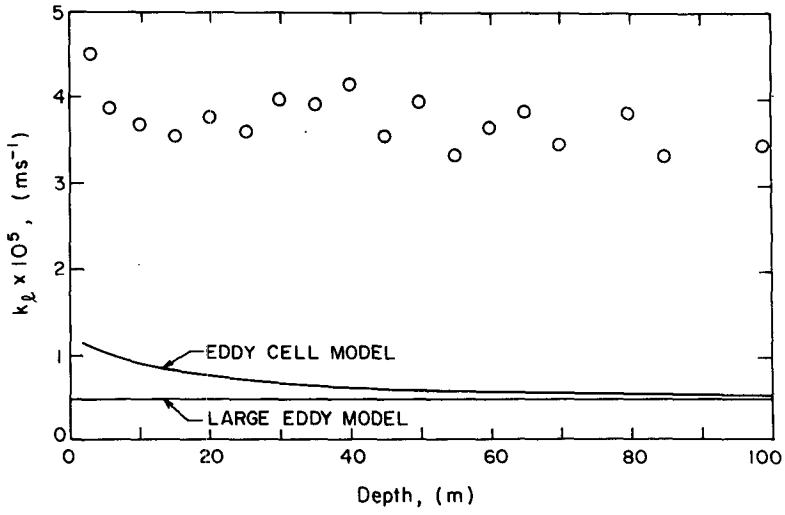

FIG. 10. Vertical liquid-phase mass-transfer-coefficient profiles from the work of Peng *et al.* (1974) and from the eddy cell and large eddy models.

The method of obtaining predictions of $k_l(z)$ follows. For both models, the physical properties were taken at 298 K for comparison to the work of Broecker and Peng (1971) and at 278 K for comparison to the work of Peng *et al.* (1974) to match the experimental conditions. The gas phase friction velocity U_* was obtained from (35), (36) and (37), using the wind speed at 10 m reported by the investigators. Neutral conditions were assumed to exist in both the atmosphere and the water in all cases. Finally, Eqs. (30) and (29) required the depth in the liquid phase at which C_l was measured and the length scale of the large eddies, respectively, as input parameters. The depths at which C_l was measured were taken from Fig. 8. The length of the eddies was taken to be 10% of the depth of the wind mixed layer because of the large total depth of the water in the areas studied.

Examining Fig. 9, we find the eddy cell model predictions are approximately a factor of 3 lower than the experimental results. The trend found for the data is very similar to the shape of the eddy cell model-prediction curve. On the other hand, the large eddy model predicts that the liquid-phase mass-transfer coefficient is constant in the vertical direction. The predictions of this model represent an average of the mass-transfer coefficient over some depth. The same observations can be made in Fig. 10, except that the eddy cell model predictions are approximately a factor of 6 less than the experimental values. Therefore, the large eddy model gives a less realistic physical picture in comparison to the data than the eddy cell model. There are many factors in the field that the models do not account for. For example, in the development of (29) and (30) it has been assumed that all the turbulence in the liquid phase is wind induced. However, if some of the turbulence were due to ocean currents, thermal instabilities and/or other convective effects, measured values of the mass-transfer coefficient would be greater than the predicted values, which is the case in Figs. 9 and 10.

The evaluation of the eddy cell and large eddy models using the data obtained from the radon method provides an opportunity to illustrate an important point. In the liquid phase, radium is decaying to radon, which subsequently decays. The models do not take these rates of decay into account. The radium decay can be neglected since it is very slow. However, the radon decay may enhance the liquid-phase mass transfer. The rates of decay of radon within the roll cell for the large eddy model and within the eddy cell for the eddy cell model can be incorporated by addition of a first-order reaction term to the diffusion equations for the respective cells. However, it has been shown that the large eddy and eddy cell models are both extensions of the surface renewal theory. In this case, one can use the results developed by Danckwerts (1951) to incorporate first-order reactions into the surface renewal model for the liquid-phase mass-transfer coefficient. Basically, if the solute undergoes a homogeneous first-order reaction within the liquid phase, Danckwerts shows that the surface renewal rate s in (7) should be replaced by $(s + \lambda_1)$. The parameter λ_1 is the reaction rate constant and for radon it is the decay constant. Therefore, the predicted mass-transfer coefficient is increased by allowing for the decay of radon in the liquid phase. For the large eddy model, s has been shown to be equal to u'/Λ and for the eddy cell model, $s = (\epsilon/\nu)^{1/2}$. The values of s for each of the investigations using the radon method have been determined for each model. The results ranged from 9.2×10^{-4} s^{-1} to

1.5 s^{-1}. The radon decay constant is equal to 2.1 $\times$ 10^{-6} s^{-1}. Comparing the values of s to the value of λ_1, one finds that the decay of radon does not significantly increase the value of k_l and can be neglected. However, this method of quantifying the effect of first-order reactions on the predictions of the models is important. For example, in a liquid with a small surface renewal rate, the reaction rate may be very significant. Or even when the surface renewal rate is large, the reaction rate can still be important for a very fast reaction. Carbon dioxide absorption by the ocean is such a case.

5. Recommendations for choice of the better model

In a new situation, it would be advantageous to know in advance which model would be expected to yield the better prediction. In the comparison to the experimental work of Fortescue and Pearson (1967), the large eddy model seemed to yield a better prediction. However, in the comparison to the field data, the eddy cell model definitely gave the better prediction. In the comparison to the experimental work of Liss (1973), the models yielded similar predictions.

One possibility of explaining this behavior is to examine Fig. 11, which is a plot of the energy spectrum function $E(n)$ in the various wavenumber ranges. As the wavenumber increases, the length scale of the eddies decreases. At low wavenumbers, the eddies are very large and permanent in nature. These eddies do not have the maximum kinetic energy due to the limited number of them present. As the wavenumber increases, the eddies are smaller. However, these eddies make the main contribution to the total kinetic energy of the turbulence and the energy spectrum reaches its maximum. Further increases in wavenumber are accompanied by increased dissipation by viscous effects. This dissipation results in a continuous decrease in the total kinetic energy. The range of high wavenumbers (small eddies) is termed "universal". Based upon the assumptions used in their derivations, the large eddy model and eddy cell model should give the better predictions of the liquid-phase mass-transfer coefficient in the energy containing eddy range and in the universal equilibrium range, respectively. Therefore, a method of determining which region of Fig. 11 characterizes the turbulence of a given situation would be helpful.

First of all, the parameter ϵ is common to these regions. In the region of energy-containing eddies, ϵ is practically equal to the energy transferred by the large eddies to the eddies of smaller scale through inertial interaction. This energy being transferred to smaller eddies can be expressed as (Hinze, 1959)

$$\epsilon = A_E u'^3/l_e, \tag{43}$$

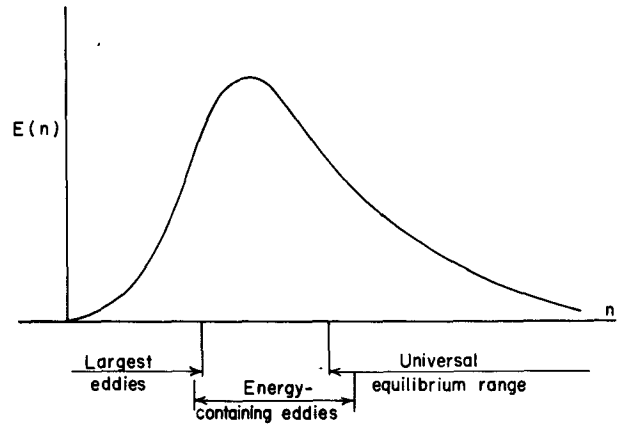

FIG. 11. Form of the energy spectrum function in the various wavenumber ranges.

where u' is the turbulent intensity, l_e the average size of the energy containing eddies and A_E a numerical constant of the order of unity. In the universal equilibrium range, ϵ is practically equal to the dissipation of energy by viscous effects. This energy dissipation can be expressed as (Hinze, 1959)

$$\epsilon = 15\nu u'^2/\lambda_g^2, \tag{44}$$

where λ_g is the length scale of the small eddies that are mainly responsible for energy dissipation.

Two appropriate Reynolds numbers can be specified from the parameters discussed above to characterize the turbulence in the regions under consideration. Hinze (1959) gives these as

$$\mathrm{Re}_l = u' l_e/\nu, \tag{45}$$

for the range of energy containing eddies and

$$\mathrm{Re}_\lambda = u'\lambda_g/\nu \tag{46}$$

for the universal equilibrium range. One can determine if an extensive equilibrium range can be expected to exist in the energy spectrum function $E(n)$. The criteria, in terms of the Reynolds numbers Re_λ and Re_l are

$$\mathrm{Re}_\lambda^{3/2} \ggg 1, \tag{47}$$

$$\mathrm{Re}_\lambda^{3/4} \ggg 1. \tag{48}$$

Therefore, either Reynolds number can be used as a determining parameter for specifying which model should be expected to yield the better prediction for a given situation.

To accomplish this, a theoretical relation between the ratio of the eddy cell model expression for k_l and that of the large eddy model involving either Re_λ or Re_l is sought. Substitution of (44) into (15) gives the eddy cell model expression for k_l as

$$k_{ls} = 0.4(D/\nu)^{1/2}\left(\frac{15\nu^2 u'^2}{\lambda_g^2}\right)^{1/4}, \tag{49}$$

where k_{ls} implies the eddy cell model prediction. Then recalling that $u' = (\overline{u^2})^{1/2}$, the ratio of the eddy cell model expression for k_l to that from the large eddy model can be obtained from (49) and (10). This ratio is

$$\frac{k_{ls}}{k_{ll}} = 0.54\left(\frac{\Lambda}{\lambda_g}\right)^{1/2}, \tag{50}$$

where k_{ll} implies the large eddy model prediction. As already discussed, both the energy-containing range and the universal equilibrium range have the parameter ϵ in common, so that (43) and (44) can be equated. Then substituting (46) and solving for the ratio of length scales yields

$$\Lambda/\lambda_g = (A_E/15)\mathrm{Re}_\lambda. \tag{51}$$

In the derivation of (51), Λ was assumed to be of the same order as l_e. Finally, substitution of (51) into (50) gives the relation for the ratio of the liquid-phase mass-transfer coefficients from the models as

$$k_{ls}/k_{ll} = 0.14(A_E\mathrm{Re}_\lambda)^{1/2}. \tag{52}$$

Rather than taking A_E equal to unity, A_E was determined using the predictions shown in Fig. 6. The rationale is that the eddy cell and large eddy model predictions shown in Fig. 6 were based on a detailed characterization of the turbulence and the theory indicated by (52) should conform to these predictions. When this was accomplished, A_E was found equal to 1.13. This value was subsequently used throughout this work.

Eq. (52) is indicated by a solid line in Fig. 12, which illustrates the dependence on the Reynolds number of the ratio of the eddy cell model prediction to the large eddy model prediction. The theoretical ratio of coefficients is equal to unity at a Reynolds number of ~45. The ratio is less than unity at lower Reynolds numbers indicating that the large eddy model would predict the higher mass transfer coefficients. Likewise, the ratio is greater than unity at higher Reynolds numbers indicating that the eddy cell model would predict the higher coefficients. However, this does not indicate which model would be expected to yield better predictions of the liquid-phase mass-transfer coefficient for a given situation. But as stated previously, an extensive universal equilibrium range would be expected to exist for large values of Re_λ or Re_l based on (47) or (48). The energy spectrum function would then exist mainly in the region of high wavenumbers and the turbulence would contain mainly small scale eddies. In this case, the eddy cell model should give the better prediction. Similarly, for small values of Re_λ or Re_l, an extensive equilibrium range would not be expected. The energy spectrum function would then exist mainly in the region of low wavenumbers and the turbulence would contain mainly large-scale eddies. In this case, the large eddy model should give the better prediction. Finally, it is reasonable to expect that at intermediate values of Re_λ or Re_l, both large and small eddies would exist. In this case, the two models should give similar results.

These expectations correspond closely to the observations made when the model predictions of liquid-phase mass-transfer coefficients were compared to the experimental evidence. For the three experimental situations previously presented, the ranges of the ratios of the eddy cell model prediction to the large eddy model prediction are indicated on Fig. 12. In the work of Fortescue and Pearson, the values of Re_λ were low and therefore it would be expected that the large eddy model predictions of k_l would not only be greater but also better than the eddy cell model predictions. This

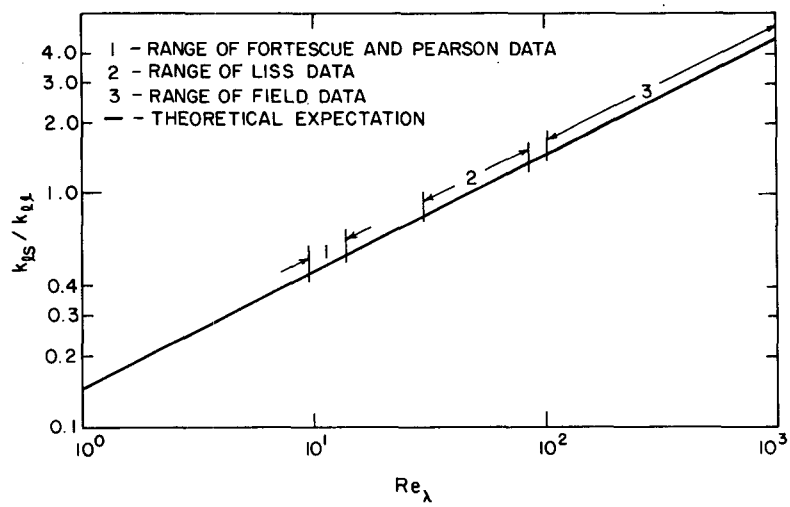

FIG. 12. Ratios of the eddy cell model prediction to the large eddy model prediction for Reynolds numbers corresponding to three experimental situations.

can be verified by examination of Fig. 6. Likewise, in the range of the field data, the values of Re_λ were high. Thus it would be expected that the eddy cell model predictions of k_l would not only be greater but also better than the large eddy model predictions. This can be verified by examination of Figs. 9 and 10. Finally, in the range of the experimental work of Liss, the values of Re_λ were intermediate and therefore it would be expected that the two model predictions of k_l should be approximately the same. This can be verified by examination of Fig. 7. Therefore, the use of Re_λ or Re_l as a criterion for choosing the better model works well for the known experimental situations and should be acceptable in determining which model would be better to use for new situations.

The quantitative recommendations for choosing which model would be expected to yield the better prediction of the liquid-phase mass-transfer coefficient for a new situation can now be presented.

The use of the large eddy model is recommended when

$$Re_\lambda < 30 \quad \text{or} \quad Re_l < 70. \tag{53}$$

The use of the eddy cell model is recommended when

$$Re_\lambda > 100 \quad \text{or} \quad Re_l > 750. \tag{54}$$

Finally, either model is recommended when

$$30 \leq Re_\lambda \leq 100 \quad \text{or} \quad 70 \leq Re_l \leq 750. \tag{55}$$

The problem involved in choosing the reference depth z for use in the eddy cell model was mentioned in connection with the comparison of the model predictions to the experimental work of Liss (1973). The method devised, discussed below, was based on the theoretical results of Fig. 12.

Using the value of l_e, which was taken equal to Λ, the Reynolds number Re_l was determined from (45). Then, using the relation given by Hinze (1959)

$$Re_l = A_E Re_\lambda^2/15, \tag{56}$$

the value of Re_λ could be obtained. The values of l_e and Re_λ were substituted into (51) to determine λ_g. Knowing λ_g permitted the determination of ϵ from (44). Finally, the value of z was obtained by substituting the value of ϵ into

$$\epsilon = w_*^3/\kappa z, \tag{57}$$

which is simply (25) under neutral conditions in the liquid phase.

The depth obtained from the procedure was plausible since it was less than the total liquid depth in the experimental situation. The procedure was not necessary in the comparison of the model predictions to the field data in Figs. 9 and 10. This is because the value of z was known from the concentration profiles in Fig. 8, making application of the eddy cell model simpler.

6. Conclusions

The exchange of gases between the atmosphere and underlying water bodies is an important mechanism by which pollutants can be removed from or added to the atmosphere. Three parameters, the gas- and liquid-phase mass-transfer coefficients and the solubility of the gas in the liquid phase, are needed to quantify this mass transfer process.

The gas solubility can be found from simple equilibrium experiments if it is not already known. The prediction of the gas-phase mass-transfer coefficient is treated in detail by Kraft (1977). Two models characterizing the turbulence in the liquid phase have been invoked to determine the liquid-phase mass-transfer coefficient. When comparing the predictions of the models to the experimental results obtained by Fortescue and Pearson (1967) in a situation in which the liquid phase turbulence was well characterized, the maximum deviation of the predictions of either model was less than a factor of 2.

Under most circumstances, it is not practical to characterize the liquid-phase turbulence in detail. Therefore, methods of approximating the input parameters for the models have been developed which yielded predictions of the liquid-phase mass-transfer coefficient within factors of 3 and 6 of experimental evidence in the laboratory and the field, respectively.

A theoretical analysis indicated that the large eddy model should give better predictions of the liquid-phase mass-transfer coefficient when the Reynolds number Re_l is less than 70. Similarly, the eddy cell model should give better predictions when Re_l is greater than 750. At intermediate values, either model is satisfactory.

With these criteria and the models, one should be able to incorporate into many pollution models the process of pollutant transfer at natural air-water interfaces. This would yield more accurate estimates of atmospheric pollutant concentrations and of the contamination of water bodies by pollutants. The resulting information should be useful in local, regional and global air and water resource management programs.

Acknowledgments. The authors gratefully acknowledge the financial support for this work provided by the Gulf Oil Foundation, administered

through the Department of Chemical Engineering at The Pennsylvania State University; and the Environmental Protection Agency via Grants R005168 and R800397, both administered through the Center for Air Environment Studies at The Pennsylvania State University.

REFERENCES

Batchelor, G. K., and A. A. Townsend, 1948: Decay of isotropic turbulence in the initial period. *Proc. Roy. Soc. London*, **193A,** 539–558.

Broecker, W. S., Y. H. Li and J. Cromwell, 1967: Radium–226 and Radon–222: Concentration in the Atlantic and Pacific Oceans. *Science*, **158,** 1307–1310.

——, and T. H. Peng, 1971: The vertical distribution of radon in the BOMEX area. *Earth Planet. Sci. Lett.*, **11,** 99–107.

Brtko, W. J., 1976: Mass transfer at natural air-water interfaces. M. S. thesis, The Pennsylvania State University, 136 pp.

Businger, J. A., J. C. Wyngaard, Y. Izumi and E. F. Bradley, 1971: Flux-profile relationships in the atmospheric surface layer. *J. Atmos. Sci.*, **28,** 181–189.

Bye, J. A. T., 1967: The wave-drift current. *J. Mar. Res.*, **25,** 95–102.

Charney, J. G., 1969: What determines the thickness of the planetary boundary layer of a neutrally stratified atmosphere? *Oceanology (Engl. Trans.)*, **9,** 111–113.

Charnock, H., 1955: Wind stress on a water surface. *Quart. J. Roy. Meteor. Soc.*, **81,** 639–640.

Danckwerts, P. V., 1951: Significance of liquid-film coefficients in gas absorption. *Ind. Eng. Chem.*, **43,** 1460–1467.

Deacon, E. L., and E. K. Webb, 1962: Small-scale interactions. *The Sea*, M. N. Hill, ed., Wiley, 864 pp.

Dobbins, W. E., 1956: The nature of the oxygen transfer coefficient in aeration systems. *Biological Treatment of Sewage and Industrial Wastes*, J. McCabe and W. W. Eckenfelder, Eds., Reinhold, 393 pp.

Dyer, A. J., and B. B. Hicks, 1970: Flux-gradient relationships in the constant flux layer. *Quart. J. Roy. Meteor. Soc.*, **96:** 715–721.

Fortescue, G. E., and J. R. A. Pearson, 1967: On gas absorption into a turbulent liquid. *Chem. Eng. Sci.*, **22,** 1163–1175.

Hanratty, T. J., 1956: Turbulent exchange of mass and momentum with a boundary. *AIChE J.*, **2,** 359–362.

Harriot, P., 1962: A random eddy modification of the penetration theory. *Chem. Eng. Sci.*, **17,** 149–154.

Hicks, B. B., 1973: The dependence of bulk transfer coefficients upon prevailing meteorological conditions. Radiological and Environmental Research Division Annual Report, ANL-8060 Part IV, Argonne National Laboratory, 98 pp.

Higbie, R., 1935: The rate of absorption of a pure gas into a still liquid during short periods of exposure. *Trans. AIChE*, **31,** 365–388.

Hinze, J. O., 1959: *Turbulence*. McGraw-Hill, 586 pp.

Kabel, R. L., 1975: Atmospheric impact on nutrient budgets. *Proc. First Specialty Symp. Atmospheric Contribution to the Chemistry of Lake Waters*, Longford Mills, Ontario, Int. Assoc. Great Lakes Res. Also *J. Great Lakes Res.*, **2,** Suppl. 1, 114–126, 1976.

King, C. J., 1966: Turbulent liquid phase mass transfer at a free gas-liquid interface. *Ind. Eng. Chem. Fundam.*, **5,** 1–8.

Kishinevsky, M. K., 1955: Two approaches to the theoretical analysis of absorption processes. *J. Appl. Chem. U.S.S.R.*, **28,** 881–886.

Kitaigorodskii, S. A., 1973: *The Physics of Air-Sea Interaction*, P. Greenburg, Ed., Israel Program for Scientific Translations, Jerusalem, 237 pp.

Kondo, J., 1976: Parameterization of turbulent transport in the top meter of the ocean. *J. Phys. Oceanogr.*, **6,** 712–720.

Kraft, R. L., 1977: Predictions of mass transfer to air-land and air-water interfaces. M. S. thesis. The Pennsylvania State University, 151 pp.

Lamont, J. C., and D. S. Scott, 1970: An eddy cell model of mass transfer into the surface of a turbulent liquid. *AIChE J.*, **16,** 513–519.

Liss, P. S., 1973: Processes of gas exchange across an air-water interface. *Deep-Sea Res.*, **20,** 221–238.

——, 1975: The exchange of gases across lake surfaces. *Proc. First Specialty Symp. Atmospheric Contribution to the Chemistry of Lake Waters*, Longford Mills, Ontario, Int. Assoc. Great Lakes Res. Also *J. Great Lakes Res.* **2,** Suppl. 1, 88–99, 1976.

Marchello, J. M., and H. L. Toor, 1963: A mixing model for transfer near a boundary. *Ind. Eng. Chem. Fundam.*, **2,** 8–12.

Monin, A. S., and A. M. Obukhov, 1954: Basic laws of turbulent mixing in the atmosphere near the ground. *Tr. Akad. Nauk SSSR, Geofiz. Inst.*, **24,** 163–187.

Munn, R. E., 1966: *Descriptive Micrometeorology*. Academic Press, 245 pp.

O'Connor, D. J., and W. E. Dobbins, 1958: Mechanism of reaeration in natural streams. *Trans. ASCE*, **123,** 641–666.

Panofsky, H. A., 1963: Determination of stress from wind and temperature measurements. *Quart. J. Roy Meteor. Soc.*, **89,** 85–94.

Peng, T. H., T. Takahashi and W. S. Broecker, 1974: Surface radon measurements in the North Pacific Ocean Station Papa. *J. Geophys. Res.*, **79,** 1772–1780.

Perlmutter, D. D., 1961: Surface-renewal models in mass transfer. *Chem. Eng. Sci.*, **16,** 287–295.

Phillips, O. M., 1966: *The Dynamics of the Upper Ocean*. Cambridge University Press, 261 pp.

Prandtl, L., 1925: Report on investigations of fully developed turbulence. *Z. Angew Math. Mech.*, **5,** 136–139.

Riley, J. P., 1971: The major and minor elements in sea water. *Introduction to Marine Chemisry*, J. P. Riley and R. Chester, Eds., Academic Press, 465 pp.

Shemdin, O. H., 1972: Wind-generated current and phase speed of wind waves. *J. Phys. Oceanogr.*, **2,** 411–419.

Sheppard, P. A., 1963: Momentum and other exchange above a water surface. *Proc. 13th Assem. IUGG-IAMP*, University of California, Berkeley, 117.

Sutton, O. G., 1953: *Micrometeorology*, McGraw-Hill, 333 pp.

Toor, H. L., and J. M. Marchello, 1958: Film-penetration model for mass and heat transfer. *AIChE J.*, **4,** 97–101.

Whitman, W. G., 1923: Preliminary experimental confirmation of the two-film theory of gas absorption. *Chem. Metall. Eng.*, **29,** 146–148.

Wu, J. 1969: Wind stress and surface roughness of air-sea interface. *J. Geophys. Res.*, **74,** 444–455.